Journal of Materials Science & Technology 205 (2025) 150–158

Contents lists available at ScienceDirect

Journal of Materials Science & Technology

journal homepage: www.elsevier.com/locate/jmst

Research Article

Fire safe and sustainable lightweight materials based on Layer-by-Layer coated keratin fibers from tannery wastes

Lorenza Abbà[a], Massimo Marcioni[a], Lorenza Maddalena[a], Guadalupe Sanchez-Olivares[b], Federico Carosio[a,*]

[a] Dipartimento di Scienza Applicata e Tecnologia, Politecnico di Torino-Alessandria Campus, Viale Teresa Michel 5, Alessandria 15121, Italy
[b] CIATEC, A.C., Omega 201, Col. Industrial Delta, León, Gto. 37545, Mexico

ARTICLE INFO

Article history:
Received 22 December 2023
Revised 29 February 2024
Accepted 16 March 2024
Available online 20 April 2024

Keywords:
Keratin fibers
Layer-by-Layer assembly
Lightweight materials
Flame retardancy

ABSTRACT

The increasing consciousness about the depletion of natural resources and the sustainability agenda are the major driving forces to try to reuse and recycle organic materials such as agri-food and industrial wastes. In this context, keratin fibers, as a waste from the tannery industry, represent a great opportunity for the development of green functional materials. In this paper, keratin fibers were surface functionalized using the Layer-by-Layer (LbL) deposition technique and then freeze-dried in order to obtain a lightweight, fire-resistant, and sustainable material. The LbL coating, made with chitosan and carboxymethylated cellulose nanofibers, is fundamental in enabling the formation of a self-sustained structure after freeze-drying. The prepared porous fiber networks (density 100 kg m^{-3}) display a keratin fiber content greater than 95 wt% and can easily self-extinguish the flame during a flammability test in a vertical configuration. In addition, during forced combustion tests (50 kW m^{-2}) the samples exhibited a reduction of 37 % in heat release rate and a reduction of 75 % in smoke production if compared with a commercial polyurethane foam. The results obtained represent an excellent opportunity for the development of fire-safe sustainable materials based on fiber wastes.

1. Introduction

In recent years, the environmental global concern and the need for a circular economy have fostered several initiatives in the development of functional materials based on natural resources [1,2]. In the insulation field, petroleum-based materials are mostly used with some sustainability and fire-safety problems [3]. The development of novel insulating materials from bio-based resources represents a great opportunity to address this problem. As well known, agricultural and food industries produce high amounts of waste, mainly in the form of fibers and fibrous materials [4,5]. Among them, keratin fibers, obtained as waste from the tannery industry, represent a good candidate for the development of bio-sourced materials.

Keratin fibers are composed of proteins called “keratins” which contain 50 % of carbon, 21 %–24 % of oxygen, 12 %–21 % of nitrogen, 6 %–7 % of hydrogen, 2 %–5 % of sulfur, and other elements [6]. Thanks to their chemical composition, keratin fibers are a durable material and, most importantly, intrinsically flame retardant [6]. Nevertheless, more than five million tons of keratin-rich wastes (including wool, hair, feathers, hooves, and horns) are generated every year by slaughterhouses and textile industries [7]. In particular, tanneries are one of the most polluting industries in the world. Solid wastes (skin trimmings, fleshes, hairs, etc.) and liquid ones are rich in chromium and sulfur and they are difficult to recycle [8,9]. Traditional disposal methods, like landfilling, composting, or incineration, represent serious environmental and health problems in the form of landscape deterioration, soil and water pollution, and the risk of transmission of pathogens [10,11]. It is thus apparent that the above-mentioned strategies represent a tremendous waste of the opportunity of reusing such a promising resource.

Within this context, the current literature on the upcycling of tannery solid wastes shows that keratin extraction from wastes is largely diffused as demonstrated by the many approaches developed for this purpose (e.g. reduction [12], oxidation [13], acid, alkali, and enzymatic hydrolysis [12,14,15], microwave irradiation [16], and ionic liquid extraction [17]). The main application of the extracted keratin is in the biomedical field for the production of

* Corresponding author.
E-mail address: federico.carosio@polito.it (F. Carosio).

https://doi.org/10.1016/j.jmst.2024.03.055

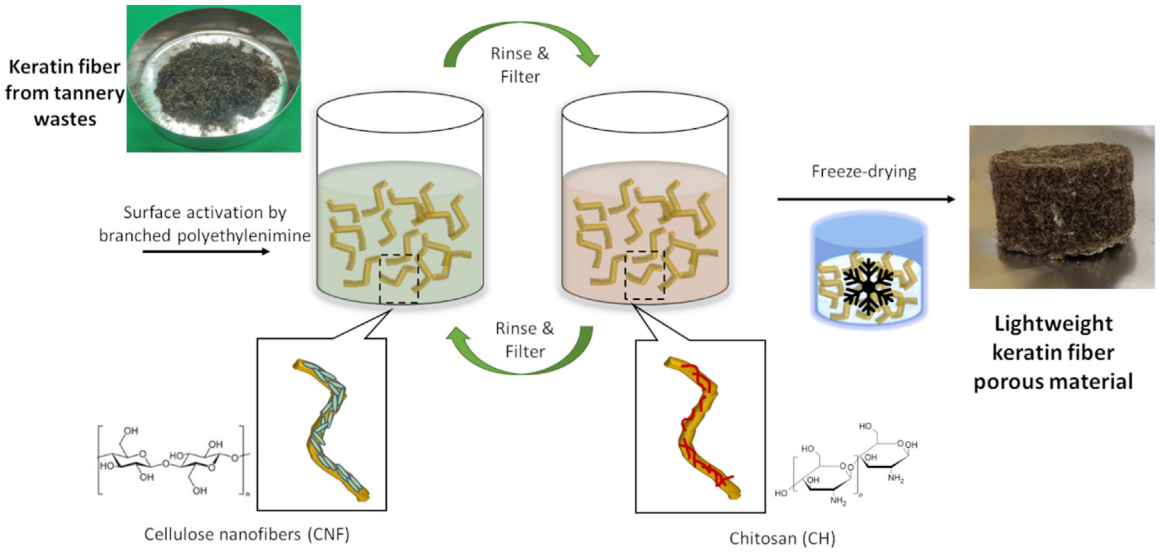

Fig. 1. Schematic representation of the approach developed in this paper. Fibers were firstly exposed to a solution of branched poly(ethyleneimine) to deposit an anchoring level. Then they were exposed alternatively to negatively charged (CNF) and positively charged (CH) baths. A rinse and filter step was performed after each layer deposition (one cycle deposit one bilayer). After the desired number of bilayers is reached, the keratin fiber network is produced by freeze-drying a water dispersion of the prepared LbL-coated fibers.

films, sponges, and scaffolds in order to mimic the structure of native tissue [18]. Thanks to the high number of polar and ionizable groups, keratin in the form of fibers has also been applied as a promising adsorbent for the removal of metal ions and toxic organic compounds [19–21].

Besides the above-mentioned applications, only a few articles can be found on the use of keratin fibers as a raw material to prepare fiber-reinforced composites. For example, Perez-Chavez et al. [22] used keratin fiber as a reinforcing agent in a biodegradable and compostable blend of corn starch and copolyester (TPS) to make a composite with flame-retardancy properties avoiding the use of toxic flame-retardancy agents. Caba's group [23] developed a bio-composite using sheep wool dispersed into a soy protein matrix with acoustic properties. Keratin fibers were also used as a filler in polyurethane foams in order to reduce flammability and improve mechanical and thermal properties [24,25]. A current limitation is represented by the quantity of fibers that can be employed. If the maximum amount is exceeded there is a deterioration of physical-mechanical properties [26]. In addition, acid and alkali environments can compromise the fiber properties leading, for example, to a decrease in strength [27,28]. This considerably limits the application of fibers as reinforcing agents for materials that are prepared under alkali conditions such as cement-based composites [29].

Stepping forward from the literature background, in this work we report an easy and green approach for the production of lightweight materials based on surface-functionalized keratin fibers derived from the tannery industry waste (Fig. 1).

The production of a stable three-dimensional (3D) structure mostly comprised of natural fibers (i.e. fiber content > 90 wt%) is a highly desirable yet challenging scientific task [30]. This is due to the limited fiber-fiber interactions that negatively impact the structural integrity of the material [31]. Attempts at producing self-standing fiber-based porous structures (herein defined as fiber networks) have been performed by Hutzler's group [32] applied a foaming process to macroscopic cellulose fibers in order to obtain a lightweight material. Wågberg's group [31] demonstrated the possibility of obtaining cellulose-based fiber networks through solvent exchange starting from self-assembled and cross-linked softwood kraft fibers. Despite some successful attempts, the use of vegetal natural fibers, such as cellulose, brings additional limitations due to their inherent flammability. This further requires additional modifications in order to meet the fire safety criteria that are mandatory for many application fields [33]. Within this context, the use of intrinsically flame-retardant animal-based fibers might represent a safer and easier alternative [34]. To the best of our knowledge, there have been no reports on the use of keratin fibers as the main building block for the development of a self-standing fiber network. To this aim, in this work, we are exploiting an approach recently developed by our research group where the Layer-by-Layer (LbL) assembly is employed as a surface nanostructuring tool capable of improving the fiber-fiber interactions and enabling the production of a porous lightweight material [35].

The main purpose of this work is therefore to present an easy and viable strategy for the upcycling of keratin fibers derived from the tannery industry waste into flame-retardant and sustainable lightweight materials capable of competing with petroleum-based foams. Chitosan (CH) and carboxymethylated cellulose nanofibers (CNF) are employed as LbL structuring polyelectrolytes. Branched polyethyleneimine (BPEI) is used as an anchoring level to improve the adhesion and homogeneity of the coating [36]. The coating assembly and fiber network production is performed in mild pH conditions that preserve the fiber properties. The presence of the coating allows the production of a porous material by ice-templating and sublimation (Fig. 1). The deposition of two or four bilayers (BLs) is enough to obtain a self-standing material. The CH/CNF LbL assembly was monitored with FT-IR spectroscopy. The morphology of the deposited coating on keratin fibers was characterized by scanning electron microscopy (SEM). The mechanical and insulating properties were evaluated through compression tests and thermal conductivity measurements. Flammability and forced combustion tests of the obtained fiber networks have been investigated by horizontal and vertical flammability tests and cone calorimetry, respectively.

2. Materials and method

2.1. Materials

Keratin fibers (hair skin bovine) were collected as waste from the beam-house stage during the tannery process of bovine leather. After being collected from a local tannery industry in Mexico, the

fibers were washed with water (150 %), ammonium sulfate, and sodium bisulfite (added at 0.5 %) in order to reduce the alkalinity from the liming process, consequently, they were drained and rinsed and the process was replicated up to obtain 7.5–8.5 pH. Afterwards, fibers were washed using surfactant products (added at 1.0 %) in order to reduce the grease from the adipose tissue. Finally, they were drained and dried in an oven at 80 °C for 24 h. Chitosan (low molecular weight, < 20,000 Da and 75 %–85 % deacetylated chitin, according to material data sheet), branched polyethyleneimine (BPEI, Mw ~25,000 Da by Laser Scattering, Mn ~10,000 by Gel Permeation Chromatography, as reported in the material datasheet) and acetic acid were purchased from Sigma Aldrich (Milwaukee, WI). Carboxymethylated cellulose nanofibers (CNF) were purchased from Rise as approx. 2% gel. CH was solubilized in 1 wt% acetic acid aqueous solution while the CNF dispersion was prepared by diluting the gel up to 0.25 wt% concentration. The so-prepared solutions and dispersions were kept under magnetic stirring overnight. The pH of CH was adjusted to 5 using a 2 M NaOH solution. BPEI was dissolved in water to 0.5 wt% concentration by means of magnetic stirring for 1 h. All the solutions were prepared with 18.2 MΩ deionized water supplied by a Q20 Millipore system (Milano, Italy).

2.2. Layer-by-Layer deposition

Prior to the LbL deposition, keratin fibers were washed with deionized water. Then, fibers were firstly dipped in BPEI solution for 10 min in order to deposit an anchoring layer. After this step, the fibers were alternately dipped in the negatively (CNF) and positively (CH) charged solutions (5 min each). Following each deposition step, to remove the excess of solution, fibers were filtered and washed by dipping in acetic acid (1 wt%) after chitosan deposition and in deionized water after CNF and BPEI deposition. A schematic representation of the vacuum filtration system used for the preparation of the fibers is shown in Fig. S1 in Supporting Information. This process was repeated until 2 and 4 bilayers were deposited. At the end of the LbL deposition, fibers were washed with water in order to remove any acetic acid remaining from the last washing. The same procedure was applied in order to evaluate the weight gain after the deposition of the CH/CNF assembly. The fibers were dried at 70 °C and weighed after the deposition of the BPEI anchoring layer (W_1) and then after the LbL deposition of the CH/CNF assembly (W_2). The weight gain was then calculated using the following equation:

$$WG(\%) = (W_2 - W_1) \times 100/W_1$$

The weight gain was 1.6 and 4.3 wt% for 2 and 4 BLs-coated fibers, respectively.

2.3. Fiber network preparation

After the deposition step, wet-coated fibers were dispersed in water and manually shaken to obtain a final fiber network density of 100 kg m^{-3}. The dispersion was poured into molds, froze for 24 h at –40 °C, and then freeze-dried for 48 h (Toption TOPT-10A, vacuum freeze dryer).

2.4. Characterization techniques

The growth of LbL assembly on model silicon wafer substrates [(100), single side polished] was monitored using Fourier transform infrared (FT-IR) spectrophotometer (16 scans and 4 cm^{-1} resolutions, Frontier, Perkin Elmer) in the transmission mode. The silicon wafer was used to monitor the growth of selected polyelectrolytes up to 5 BLs by using static dipping following the same procedure used for fibers (in terms of layer sequence and deposition times). After each deposition step, the Si wafer was dried and IR spectra of the deposited layer were collected. Attenuated total reflectance (ATR) FT-IR spectroscopy spectra for neat and coated keratin fibers were collected, at room temperature, in the range of 4000–700 cm^{-1} (16 scans and 4 cm^{-1} resolution) using an FT-IR spectrophotometer (Frontier, Perkin Elmer, Italy) equipped with germanium crystal.

Surface morphology of untreated and LbL-treated fibers and 3D networks before and after the cone calorimetry test was investigated using Scanning Electron Microscopy (SEM) on a ZEISS, EVO 15 model. The samples were placed on a small piece of adhesive tape and gold-metalized.

Mechanical properties were evaluated using a dynamometer (Instron 5966, 2 kN cell, Canton, MA) by compressing cylindrical samples of approx. 30 mm diameter and 20 mm height between two horizontal plates at a constant rate of 10 mm min^{-1}. The compressive modulus was calculated from the initial liner section of the compression curves (between 2 %–5 % compression strain). Before the tests, samples were conditioned at 23.0 ± 0.1 °C and 50.0 ± 0.1 RH for 48 h in a climatic chamber.

The isotropic thermal conductivity was evaluated by a transient plane heat source method (ISO 22,007–2) using the TPS 2500S instrument by Hot Disk AB (Göteborg, Sweden) equipped with a Kapton sensor (radius 6.403 mm). The measuring setup was inserted in a container dipped into a silicone oil bath (Haake A40, Thermo Scientific Inc., Waltham, MA, USA) supplied with a temperature controller (Haake AC200, Thermo Scientific Inc., Waltham, MA, USA) in order to control the temperature at 23.00 ± 0.01 °C. The samples were produced in a square shape 5 mm × 5 mm and 5 mm thickness. Before testing, the samples were stored in a climatic chamber at 23.0 ± 0.1 °C and 50.0 % ± 0.1 % R.H. for at least 24 h.

Thermal stability was evaluated by TGA (Discovery, TA Analysis). The samples (approx. 5 ± 1 mg) were placed into alumina pans and subjected to an isothermal treatment for 30 min at 100 °C in order to remove moisture then the temperature was increased to 700 °C at 10 °C min^{-1}. The test was performed both in nitrogen and air atmosphere. T_{onset} (temperature corresponding to 2 % weight loss), T_{max} (temperature at maximum rate of weight loss), and residue (%) were obtained by these measurements.

The flammability of samples was tested both in horizontal and vertical configurations. The sample (50 mm × 15 mm × 15 mm) was ignited from its short side by a 20 mm blue methane flame (flame application: 2 × 6 s). The test was repeated at least two times for each formulation to ensure reproducibility. The ability to stop flame spread and final residue (%) were evaluated.

Cone calorimetry (GA01, ISO 5660, Noselab Ats, Italy) was employed to investigate the combustion behavior of untreated and LbL-treated samples (50 mm × 50 mm × 15 mm) under 50 kW m^{-2} heat flux. The following parameters were registered: Time to Ignition (TTI, (s)), peak of Heat Release Rate (pkHRR, (kW m^{-2})), Total Heat Release (THR, (MJ m^{-2})), Smoke Production Rate (SPR, (m^2 s^{-1})), Total Smoke Release (TSR, (m^2 m^{-2})) and final residue (%). The test was repeated 3 times for each formulation and the experimental error was assessed as the standard deviation (σ). Prior to cone calorimetry and flammability tests, samples were conditioned in a climatic chamber (23.0 ± 0.1 °C, 50.0 % ± 0.1 % R.H.) for at least 48 h.

3. Results and discussion

3.1. Coating growth and morphology

The LbL growth assembly of the CH/CNF system, up to 5 BLs, was first evaluated by FT-IR spectroscopy on a model silicon substrate following the procedure described in the materials and

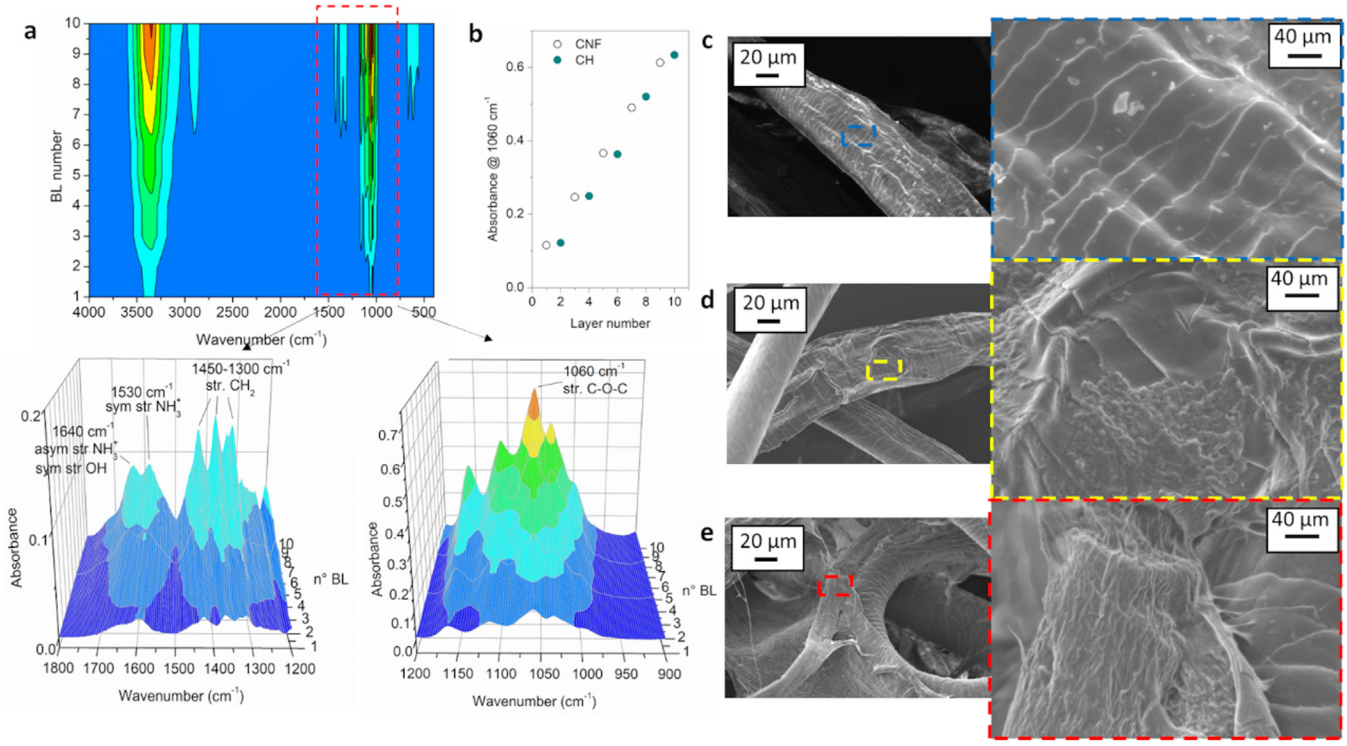

Fig. 2. Characterization of the layer-by-layer growth of CH/CNF on Si wafer and surface morphology on keratin fibers: (a) 3-D projection (b) intensity of the signal at 1060 cm^{-1} as the function of the layer number, (c) SEM images of neat keratin fiber, (d) 2BLs and (e) 4BLs-coated fibers.

method section. The spectra of neat CH and CNF were collected as well (Fig. S2). Chitosan shows a broad band between 3700 and 3000 cm^{-1} related to the stretching vibration of –OH groups (ascribed to CH and residual water) overlapping with the stretching of amine groups (3550–3330 cm^{-1}). Between 2900 and 2870 cm^{-1} are visible signals of the C–H bond in CH_2 and CH_3 respectively. The most intense signal, at 1074 cm^{-1}, is related to C–O–C stretching vibration [37–39]. The characteristic peaks of protonated amine groups are at 1650 cm^{-1} (asymmetric stretching) and 1530 cm^{-1} (symmetric stretching) [37]. CNF's most intense band at 1060 cm^{-1} is related to C–O–C pyranose ring stretching vibration. The carboxylic group absorbs at 1610 cm^{-1} while the vibrations of CH and CH_2 are clearly visible between 1400 and 1300 cm^{-1} [40]. Fig. 2(a, b) shows the 3-D plot of spectra collected during the build-up on the silicon wafer and the intensity vs $n°$ of the layer deposited for characteristic CH and CNF peaks. The intensity of the C–O–C absorbance signal grows proportionally to the BLs deposited thus suggesting the successful assembly of the components. The intensity of the peak at 1060 cm^{-1} displays a linear growth where the adsorption of CNF produces a steep increase in the absorbance thus suggesting this latter as the main component of the coating (Fig. 2(b)). This observation is supported by a previously published study evaluating the LbL assembly of a CH/phosphorylated-CNF by FT-IR and quartz crystal microbalance [39].

The $[CNF/CH]_n$ coating was then transferred to keratin fibers by depositing $n = 2, 4$ bilayers as described previously in the methodology section. To investigate the surface morphology of the samples scanning electron microscopy was employed. Untreated- and 2–4 BLs-treated fibers are displayed in Fig. 2(c–e). Neat keratin fibers display irregular shapes and a smooth surface morphology. The external layer of the fiber, the cuticle, is made of flat and partially overlapped cells [41,42]. The performed LbL deposition leads to the formation of thin CH/CNF assemblies that produce spots characterized by a fibrous morphology. Increasing the number of bilayers to 4 BLs leads to an increase in the surface coverage.

3.2. Fiber network structure and mechanical properties

A water dispersion of LbL-treated keratin fibers was freeze-dried in order to obtain a self-standing fiber network. Fig. 3 shows digital images of the fiber network, SEM investigation of samples prepared from 4 BLs-coated fibers, and a schematic representation of the fiber network formation upon freeze-drying.

The produced fiber network can be handled and can withstand the load of a static weight of 200 gr without being deformed, as reported in Fig. 3(a). SEM images of the microstructure evidence that physical interaction between fibers ensures the structural integrity of the network (Fig. 3(b)). Higher magnifications reveal the formation of bridges between the keratin fibers thanks to the interpenetration of the deposited coating that acts like a glue that keeps the fibers together. Similar joints are also detected for samples prepared from 2 BLs-coated fibers (Fig. S3). It is worth highlighting that it is not possible to produce such a 3-D network with uncoated fibers as after the freeze-drying process the resulting structure is extremely brittle and collapses on itself when removed from the mold (Fig. S4). This result suggests the fundamental role of the LbL coating in the formation mechanism of the fiber network (Fig. 3(c)). During freezing, the ice crystals nucleation and growth push the LbL-coated fibers together producing entanglements. In this way, structural joints are formed between touching hydrated CH/CNF assemblies. Upon ice sublimation, such joints consolidate and confer the structural integrity needed for the formation of a stable fiber network.

The mechanical properties have been assessed by compression tests while the thermal insulating characteristics were measured in terms of thermal conductivity. Fig. 4 reports the compression stress-strain curves for 2 and 4 BL samples and a comparison of the measured thermal conductivity values with reference materials from the literature background [43–45].

Stress-strain curves, in Fig. 4(a), show a linear behavior at low deformation (< 2 %), then the samples progressively collapse and

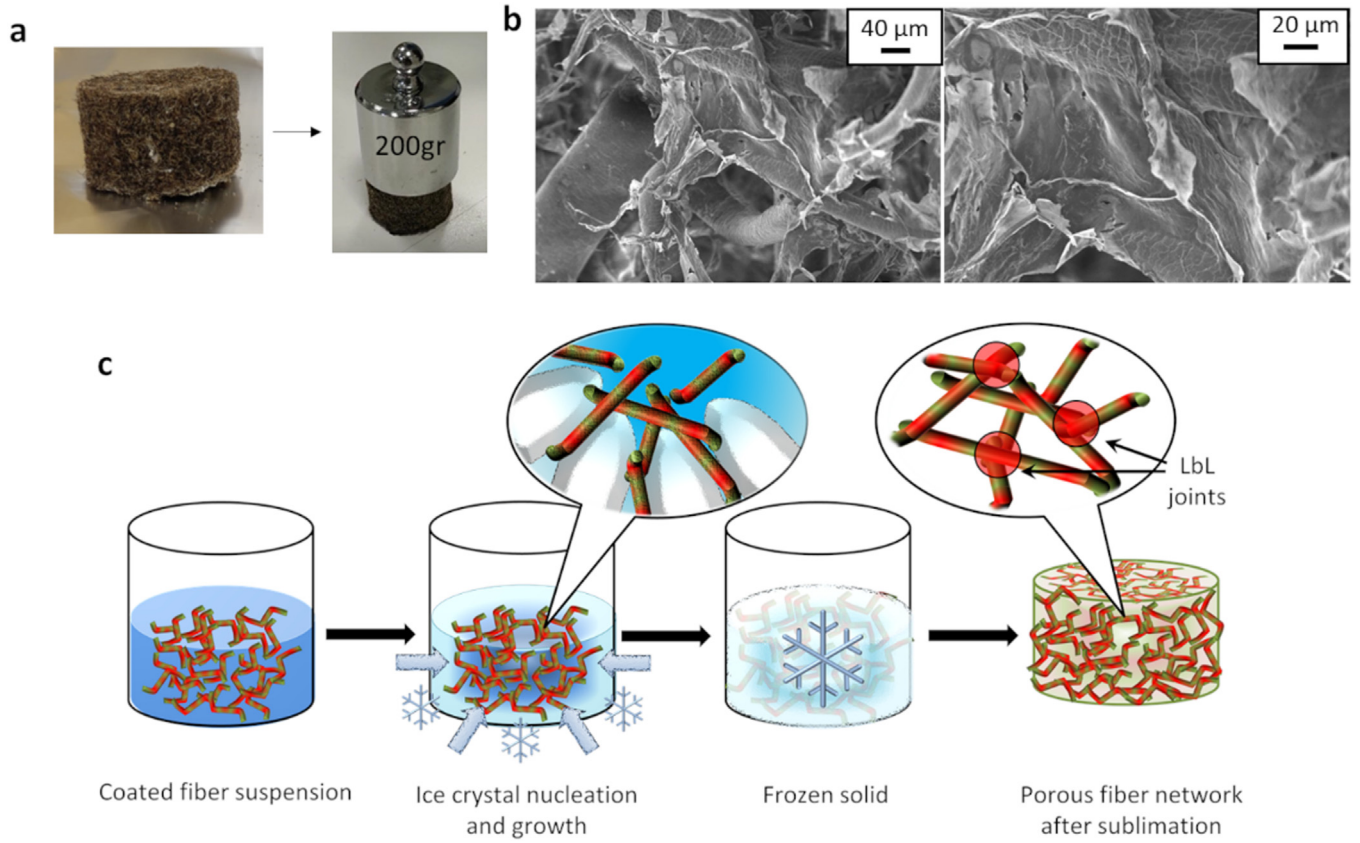

Fig. 3. Fiber network characterization: (a) digital images of the prepared fiber network, (b) SEM images of the 4BL network, (c) schematization of the formation mechanism of the porous network by freeze-drying.

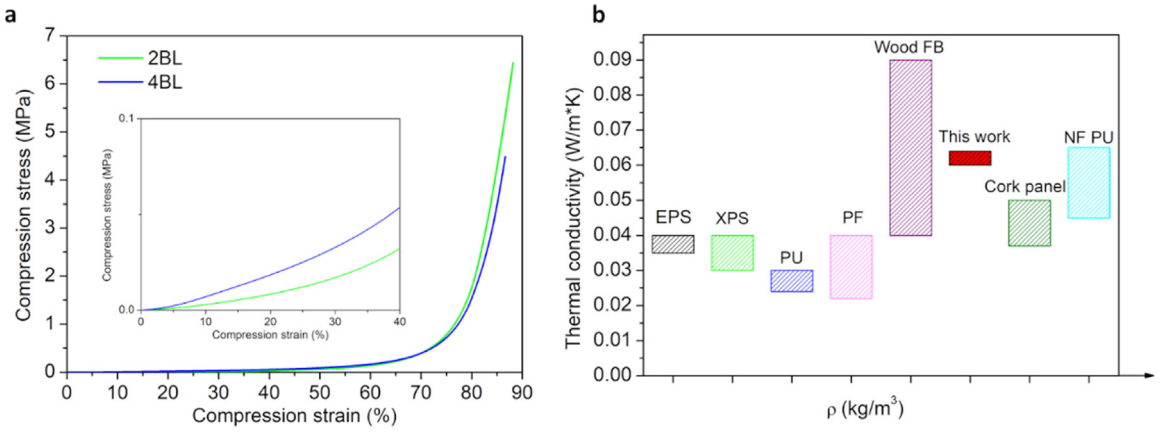

Fig. 4. Functional fiber network characterization: (a) compression stress-strain curves for 2 and 4 BL fibers networks with a magnification in the compression range 0–40 %, (b) comparison of thermal conductivity of different materials from the literature background. EPS: expanded polystyrene (15–35 kg m^{-3}), XPS: extruded polystyrene (25–45 kg m^{-3}), PU: polyurethane foam (30–100 kg m^{-3}), PF: phenolic foam (40–110 kg m^{-3}), Wood FB: wood fiberboard (30–270 kg m^{-3}), Cork Panel (110–170 kg m^{-3}), NF PU: natural fiber reinforced PU (105–178 kg m^{-3}).

reach, at high deformations (> 70 %), a step of densification typical of conventional rigid foams [45]. Compressive modulus, calculated from the initial linear behavior, is about 19.0 ± 6.5 and 31.0 ± 6.7 KPa for 2 and 4 BL fiber networks, respectively. The values measured are inferior to the ones obtained for a similar porous structure based on self-assembled and crosslinked cellulose fibers [31].

This could be ascribed to the reduced add-on of the coating that only comprises 1.6 and 4.3 % of the fiber network at 2 and 4 BLs, respectively. In addition, the broad size distribution of the employed keratin fibers, that are collected from tannery waste, likely resulted in a limited formation of functional fiber-fiber entanglements during freeze-drying (schematically represented in Fig. 3(c)). These two effects resulted in a reduced density of LbL structural joints that, while being capable of yielding a sTable 3D structure, had limited effects on the compressive strength of the prepared materials. The thermal conductivity values were found to be 0.060 ± 0.005 and 0.064 ± 0.005 W m^{-1} K^{-1} for 2 and 4 BL fiber networks, respectively. These values are below the threshold of 0.065 W m^{-1} K^{-1} which is normally considered as the upper limit for thermal insulating materials [34]. When compared with other materials from the literature background (Fig. 4(b)), the measured values are higher than the thermal conductivities of tradi-

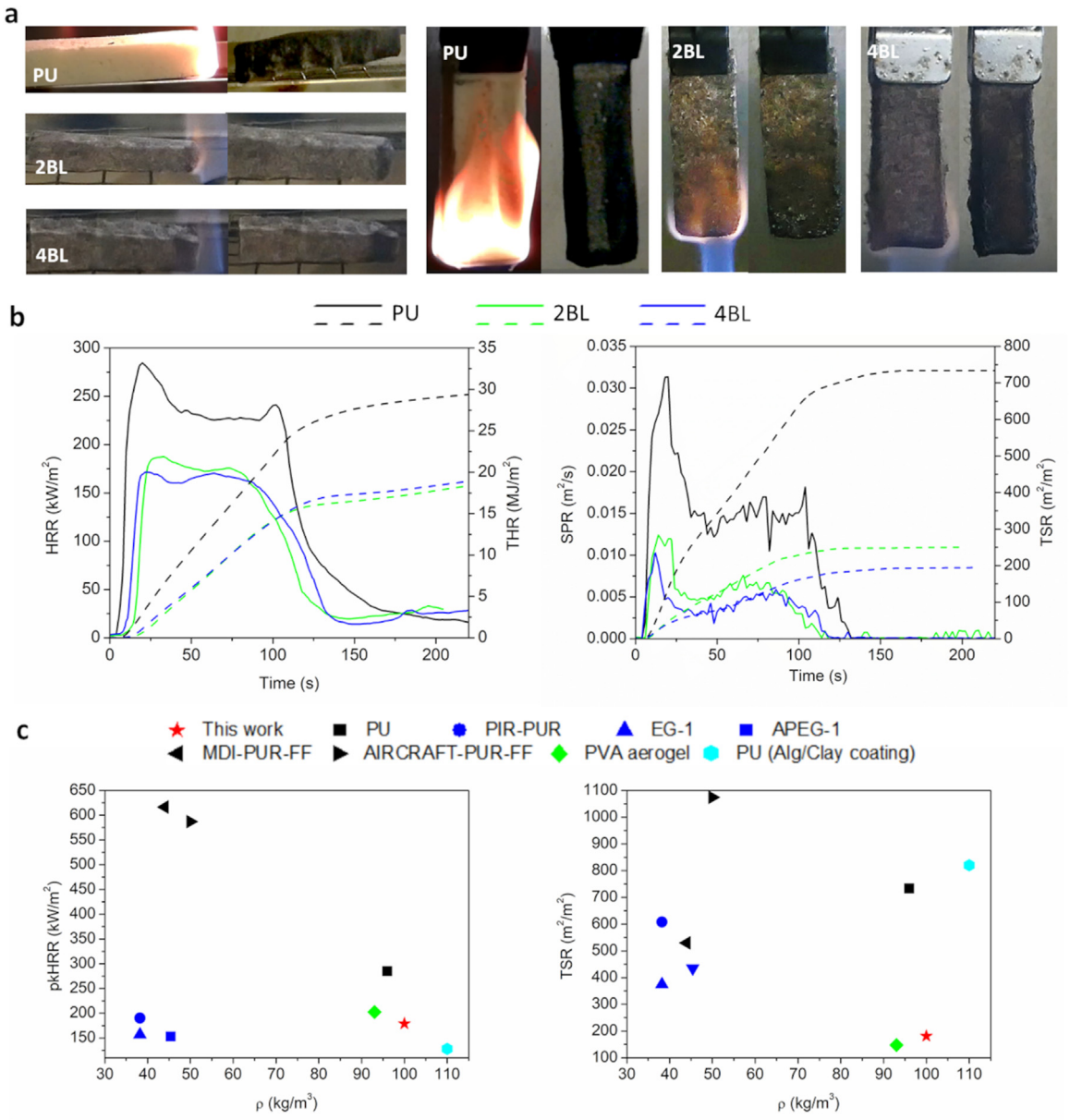

Fig. 5. Flame retardant characterization of prepared fiber networks: (a) Snapshots taken during flammability test in the horizontal and vertical configuration for commercial PU, 2 and 4 BL networks; (b) cone calorimetry plot of heat release rate (HRR) and total THR on the left and SPR and TSR on the right; (c) comparison of cone calorimetry results of different foam from the literature background. PIR-PUR: polyisocyanurate-polyurethane foam, EG-1: PIR-PUR foam with expandable graphite, APEG-1: PIR-PUR foam with ammonium phosphate and expandable graphite, MDI-PUR-FF, AIRCRAFT-PUR-FF: commercial PU foams, PVA aerogel: poly(vinylalcohol) aerogel, PU (Alg/Clay coating): PU with surface coating made with alginate and clay aerogel).

tional non-renewable porous materials but comparable to the ones of natural materials that are currently used for the fabrication of fiber-filled polyurethanes and fiberboards for the construction sector. This finding suggests that the fiber networks developed in this paper could be applied as lightweight insulating panels where no load-bearing function is needed.

3.3. Thermal and thermo-oxidative stability

The thermal decomposition of neat and coated keratin fibers was investigated by thermogravimetric analysis in nitrogen and air atmospheres. The aim is to evaluate whether the fiber network production process and the LbL-assembled coating modified the thermal and thermo-oxidative stability of the fibers. Fig. S5 reports the weight and derivative weight plots as a function of temperature while Table S1 discloses the collected data. In the inert atmosphere, the keratin fibers decompose in a single step that starts at 234 °C with a maximum weight loss rate at 309 °C and leads to the formation of a thermally stable residue that accounts for 23 wt% of the initial weight. As reported in the literature, the decomposition path involves different overlapping steps that are linked to the keratin hierarchical structure and chemical composition [46,47]. NH_3 and CO_2 are the main products released below 300 °C in combination with sulfur-containing compounds while nitriles and phenol-base compounds are released above 300 °C [48]. The process yields O, N, and S-rich thermally stable charred structures [49]. In the air, the first decomposition step occurs in the same temperature range observed in nitrogen. Then, the oxidation of the charred residue produced from the former step results in a second weight loss in the 500–650 °C range [50]. Keratin fiber networks produced from

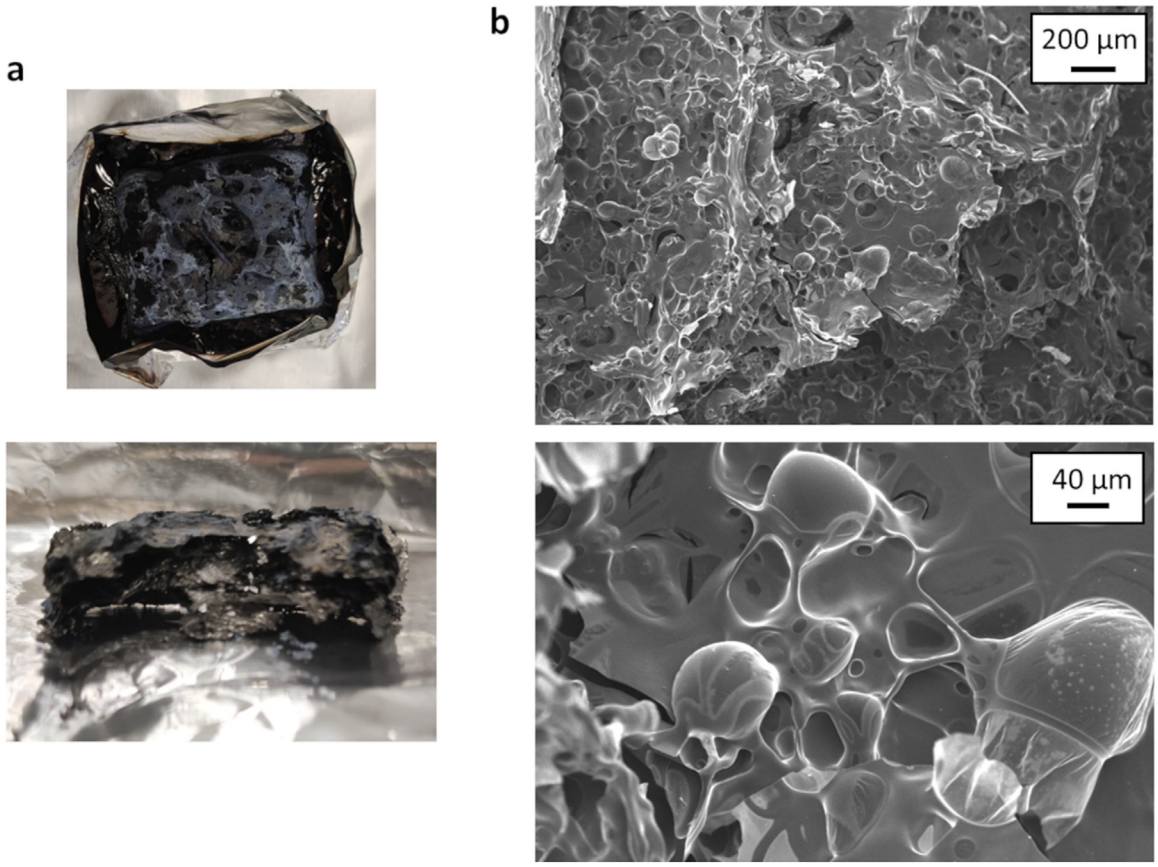

Fig. 6. Residue analysis of 4 BL network after cone calorimetry test: (a) digital photos of residue; (b) SEM images.

2 to 4 BLs-coated fibers yield nearly superimposable TG plots thus highlighting that the deposition of the CH/CNF coating did not impact the fiber thermal and thermo-oxidative stability.

3.3. Flammability and forced combustion tests

To evaluate flame retardant properties of the prepared fiber networks, flammability, and cone calorimetry tests were performed. The former evaluates the ability of the material to start a fire by exposure to a direct flame [51]. The latter evaluates the behavior of a material during a fire by exposing the specimen to a heat flux typically found in the early stages of developing fires [52]. These two tests provide a complementary set of reactions to fire characterization. Fig. 5 displays the snapshots of the samples taken during the flammability test both in horizontal and vertical configuration and cone calorimetry HRR and SPR vs-time plots along with their integral values and a comparison of the measured pkHRR and TSR values with materials from the literature background [53–56]. A commercially available PU foam having a density similar to the prepared keratin fiber networks is employed for comparison. The data from the flammability test and cone calorimetry are collected in Tables S2 and S3, respectively.

Flammability in horizontal setup was first evaluated (Fig. 5(a)). Upon the methane flame application, both 2 and 4 BL samples exhibit the same behavior: no flame spread occurs and the flame self-extinguishes immediately after the removal of the methane igniter thus resulting in a non-igniting behavior (after flame time = 0 s). As a consequence, almost the totality of the samples remains intact with residues above 90 % (Table S2). The same behavior is displayed by a loose mat of neat keratin fibers thus highlighting how the presence of the LbL coating did not alter their intrinsic FR characteristics (Fig. S6). In addition, the vertical test was also performed. This configuration represents a more severe testing condition if compared to the horizontal one and it is typically considered a fundamental test to evaluate the flammability of dense materials. Similarly to what was observed during horizontal tests, also in this setup, all specimens display a non-igniting behavior where the flame immediately self-extinguished after the removal of the ignition source. In strong contrast, the commercial PU can't stop flame propagation and burns completely in both horizontal and vertical configurations (Fig. 5(a)). A cone calorimetry test was performed to investigate sample behavior under a 50 kW m^{-2} heat flux which simulated a well-developed fire scenario and represents a more severe testing condition than the usually adopted 35 kW m^{-2} [52]. It is worth highlighting that 50 kW m^{-2} was selected since under 35 kW m^{-2} the keratin fiber networks exhibited a mixed igniting/non-igniting behavior with limited reproducibility. During a cone calorimetry test, the material starts decomposing upon exposure to the applied heat flux and it releases volatile products that ignite when the concentration limit is reached, leading to the flaming combustion of the sample. The above-mentioned mixed behavior under 35 kW m^{-2} therefore suggests the release of flammable volatiles close to the lower flammability limits [57]. Conversely, under 50 kW m^{-2} ignitions occurred for all the tested keratin fiber networks that ignite after an average of 10 s and burn with extensive charring. This helps in keeping the structural integrity of the samples that maintain their original shape at the end of the test. During combustion 2 and 4 BL samples yield pkHRR values of 194 and 179 kW m^{-2} which are 32 % and 37 % less than the reference rigid PU foam tested (Fig. 5(b), Table S3). Interestingly, total smoke release (TSR) values achieved from keratin fiber networks are very low if compared with the ref-

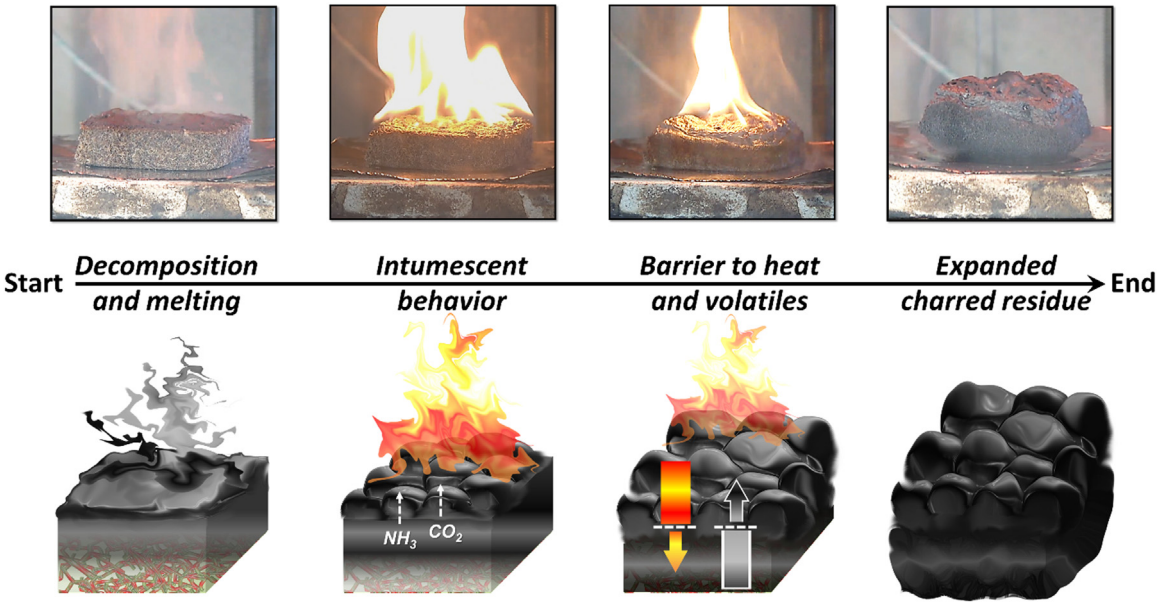

Fig. 7. Schematic representation of the keratin fiber network reaction to the exposure to a flame or a heat flux.

erence PU samples (i.e. 181.2 and 733.5 m^2 m^{-2} for the 4 BL and PU, respectively). Smoke production is an important hazard parameter in many fire-related situations. Since smoke particulate opacity and inhalation are considered a major cause of fire deaths [58], the low values of TSR measured point out the fire-safety potentiality of the keratin fibers networks. A comparison with the literature background further highlights the excellent FR properties of the prepared materials that, differently from other FR solutions, can combine low combustion rates with extremely reduced smoke production (Fig. 5(c)).

3.4. Post-combustion residue investigation

Post-combustion residues collected after cone calorimetry tests were characterized by SEM investigations. Fig. 6 exhibits digital images of 4 BL residues and SEM observations at different magnifications. Digital images and SEM characterizations of 2 BL residues are shown in Fig. S7.

After combustion, the fiber network prepared from coated fibers produces a self-standing residue that can easily be handled. SEM images display an expanded structure characterized by bubbles in which fibers cannot be distinguished anymore. This structure is typical of an intumescent system, the char formation involves all the specimens, and it is mainly ascribed to the keratin fibers behavior. Indeed, it is well known that wool has intrinsically low flammability due to high nitrogen and sulfur content in the amino acid skeleton [59]. An analogous mechanism has been proposed for the combustion of keratin fiber derived from industrial wastes [48].

Based on the performed characterization and the literature background on keratin thermal decomposition it is possible to preliminarily discuss a FR mechanism for the prepared keratin fiber networks (Fig. 7).

The keratin fibers directly exposed to a flame or a heat flux initially decompose and melt releasing volatiles while producing a layer of a low viscosity liquid [60]. This latter is expanded by CO_2 and NH_3 that are released by the underneath keratin fibers upon early-stage decomposition [48]. This produces an intumescent charred layer on the surface of the burning fiber network [61]. Simultaneously, the CH/CNF assembly undergoes extensive charring with the formation of dense charred structures that confer structural stability to the network upon keratin fibers' intumescence [39,62–64]. This observation is supported by previously published results where coatings comprising CH/CNF assemblies were found capable of preventing the collapsing of flexible PU foams during combustion [39]. This combined action leads to the formation of a thermal barrier at the sample/flame interface that produces favorable reductions in heat transfer and release of decomposition products. In this way, the amount of volatiles that feed the flame is progressively reduced leading to the observed self-extinguish behavior during flammability test and low heat and smoke release during cone calorimetry. The structure keeps on expanding until combustion ends leaving a residue almost twice the height of the original sample.

4. Conclusions

In this work, lightweight and fire-safe materials have been produced from Layer-by-Layer coated keratin fibers from the tannery industry waste. Chitosan and nanocellulose were selected as LbL coating constituents. The coating growth was evaluated on model Si wafer substrate pointing out a linear growth regime yielding nanocellulose-rich assemblies. Fibers coated with 2 or 4 BLs were employed to produce porous fiber networks by means of ice-templating and sublimation processes. The coating acted like a glue enhancing fiber-fiber interaction and enabling the formation of a self-standing 3D structure upon template removal. By the same templating procedure, uncoated fibers collapsed into brittle aggregates. Conversely, fiber networks produced from LbL-coated fibers display good structural integrity allowing them to withstand the compression of a static weight without being deformed. The thermal conductivity values were found to be below 0.065 W m^{-1} K^{-1}, which represents the threshold for thermal insulating materials. The flame retardant characterization pointed out how these fiber networks can easily self-extinguish the flame during flammability tests while simultaneously displaying low heat release rates and total smoke release by forced combustion tests, an overall FR performance hardly displayed by state-of-the-art materials. These excellent results are ascribed to the intrinsic flame retardant features of the keratin fibers that are capable of producing intumescent-like structures when exposed to a flame or a heat flux as pointed out by post-combustion residue investigations by SEM.

The so produced barrier limits the amount of combustible volatiles fueling the flame thus producing the observed self-extinguishing behavior and low heat and smoke release. Further development might be focused on changing the composition of the coating in order to target specific flame retardancy or improved mechanical properties. In conclusion, the proposed approach can be considered an efficient way for the upcycling of keratin fiber wastes into green and functional materials characterized by excellent fire safety and low environmental impact.

Declaration of competing interest

The authors declare that they have no known competing financial interests or personal relationships that could have appeared to influence the work reported in this paper.

Acknowledgements

The authors thank Dario Pezzini for SEM acquisitions. This work was supported by the Italian Ministry of University (MIUR) call PRIN 2017 with the project “PANACEA: A technology Platform for the sustainable recovery and advanced use of NAnostructured CEllulose from Agro-food residues” (grant No. 2017LEPH3M).

Supplementary materials

Supplementary material associated with this article can be found, in the online version, at doi:10.1016/j.jmst.2024.03.055.

References

[1] E.C.D. Tan, P. Lamers, Front. Sustain. 2 (2021) 701509.
[2] M. Cavallo, D. Cencioni, Circular Economy, Benefits and Good Practices, Edizioni Ambiente, Milano, Italy, 2017.
[3] N.V. Gama, A. Ferreira, A. Barros-Timmons, Materials (Basel) 11 (2018) 1841.
[4] E. Papadopoulou, D. Bikiaris, K. Chrysafis, M. Wladyka-Przybylak, D. Wesolek, J. Mankowski, J. Kolodziej, P. Baraniecki, K. Bujnowicz, V. Gronberg, Ind. Crops. Prod. 68 (2015) 116–125.
[5] N. Reddy, Y. Yang, Trends Biotechnol. 23 (2005) 22–27.
[6] F. Allafi, M.S. Hossain, J. Lalung, M. Shaah, A. Salehabadi, M.I. Ahmad, A. Shadi, J. Nat. Fibers 19 (2022) 497–512.
[7] M. Zoccola, A. Aluigi, C. Tonin, J. Mol. Struct. 938 (2009) 35–40.
[8] S.K. Verma, P.C. Sharma, Crit. Rev. Biotechnol. 43 (2023) 805–822.
[9] S. Gupta, S. Gupta, P. Dhamija, S. Bag, Benchmarking 25 (2018) 797–814.
[10] C. Chaitanya Reddy, I.A. Khilji, A. Gupta, P. Bhuyar, S. Mahmood, K.A. Saeed AL-Japairai, G.K. Chua, J. Water Process. Eng. 40 (2021) 101707.
[11] I. Chukwunonso Ossai, F. Shahul Hamid, A. Hassan, Waste Manage. 151 (2022) 81–104.
[12] I. Sinkiewicz, A. Śliwińska, H. Staroszczyk, I. Kołodziejska, Waste Biomass. Valorization 8 (2017) 1043–1048.
[13] K. Fukatsu, Sen'i Gakkaishi 53 (1997) 167–170.
[14] C. Vineis, A. Varesano, G. Varchi, A. Aluigi, in: S. Sharma, A. Kumar (Eds.), Keratin as a Protein Biopolymer, Springer International Publishing, Cham, Switzerland, 2019, pp. 35–76.
[15] C.R. Chilakamarry, S. Mahmood, S.N.B.M. Saffe, M.A. Bin Arifin, A. Gupta, M.Y. Sikkandar, S.S. Begum, B. Narasaiah, Biotech 11 (2021) 220.
[16] M. Zoccola, A. Aluigi, A. Patrucco, C. Vineis, F. Forlini, P. Locatelli, M.C. Sacchi, C. Tonin, Text. Res. J. 82 (2012) 2006–2018.
[17] H. Xie, S. Li, S. Zhang, Green Chem. 7 (2005) 606–608.
[18] J.G. Rouse, M.E. Van Dyke, Materials (Basel) 3 (2010) 999–1014.
[19] A. Aluigi, F. Rombaldoni, C. Tonetti, L. Jannoke, J. Hazard. Mater. 268 (2014) 156–165.
[20] G. Freddi, T. Arai, G.M. Colonna, A. Boschi, M. Tsukada, J. Appl. Polym. Sci. 82 (2001) 3513–3519.
[21] M. Sulyman, J. Namiesnik, A. Gierak, Int. J. Adv. Sci. Eng. Technol. 5 (2017) 2321–9001.
[22] R. Pérez-Chávez, J. Sánchez-Aguilar, F. Calderas, L. Maddalena, F. Carosio, G. Sanchez-Olivares, Polym. Degrad. Stabil. 201 (2022) 109991.
[23] M. Urdanpilleta, I. Leceta, P. Guerrero, K. de la Caba, Polymers (Basel) 14 (2022) 5231.
[24] S. Członka, N. Sienkiewicz, A. Strąkowska, K. Strzelec, Polym. Test. 72 (2018) 32–45.
[25] K. Wrześniewska-Tosik, J. Ryszkowska, T. Mik, E. Wesołowska, T. Kowalewski, M. Pałczyńska, K. Sałasińska, D. Walisiak, A. Czajka, Polymers (Basel) 12 (2020) 2943.
[26] I. Aranberri, S. Montes, I. Azcune, A. Rekondo, H.J. Grande, Polymers (Basel) 10 (2018) 1056.
[27] E. Vernon Truter, Introduction to Natural Protein Fibres: Basic Chemistry, 1973.
[28] M. Alzeer, K.J.D. MacKenzie, J. Mater. Sci. 47 (2012) 6958–6965.
[29] D. Jóźwiak-Niedźwiedzka, A.P. Fantilli, Materials (Basel) 13 (2020) 3590.
[30] E.S. Ferreira, C.A. Rezende, E.D. Cranston, Green Chem. 23 (2021) 3542–3568.
[31] V. Lopez, J. Erlandsson, L. Wågberg, P. Larsson, ACS Sustain. Chem. Eng. 6 (2018) 9951–9957.
[32] S.R. Burke, M.E. Möbius, T. Hjelt, S. Hutzler, Cellulose 26 (2019) 2529–2539.
[33] O. Köklükaya, F. Carosio, V.L. Durán, L. Wågberg, Carbohydr. Polym. 230 (2020) 117468.
[34] O. Dénes, I. Florea, D.L. Manea, Procedia Manuf. 32 (2019) 236–241.
[35] M. Marcioni, M. Zhao, L. Maddalena, T. Pettersson, R. Avolio, R. Castaldo, L. Wågberg, F. Carosio, ACS Appl. Mater. Interfaces 15 (2023) 36811–36821.
[36] A.A. Cain, M.G.B. Plummer, S.E. Murray, L. Bolling, O. Regev, J.C. Grunlan, J. Mater. Chem. A 2 (2014) 17609–17617.
[37] G. Socrates, Infrared and Raman Characteristic Group Frequencies. Tables and Charts, 3rd ed, Wiley, Hoboken, USA, 2001.
[38] B. Gieroba, A. Sroka-Bartnicka, P. Kazimierczak, G. Kalisz, A. Lewalska-Graczyk, V. Vivcharenko, R. Nowakowski, I.S. Pieta, A. Przekora, Int. J. Mol. Sci. 23 (2022) 5953.
[39] F. Carosio, M. Ghanadpour, J. Alongi, L. Wågberg, Carbohydr. Polym. 202 (2018) 479–487.
[40] R. Rai, P. Dhar, Nanotechnology 33 (2022) 362001.
[41] S. Perța-Crișan, C. Ștefan Ursachi, S. Gavrilaș, F. Oancea, F.D. Munteanu, Polymers (Basel) 13 (2021) 1896.
[42] B.S. Lazarus, C. Chadha, A. Velasco-Hogan, J.D.V Barbosa, I. Jasiuk, M.A. Meyers, IScience 24 (2021) 102798.
[43] L.D. Hung Anh, Z. Pásztory, J. Build. Eng. 44 (2021) 102604.
[44] S. Schiavoni, F. D'Alessandro, F. Bianchi, F. Asdrubali, Renew. Sust. Energ. Rev. 62 (2016) 988–1011.
[45] H. Shao, Q. Zhang, H. Liu, W. Guo, Y. Jiang, L. Chen, L. He, J. Qi, H. Xiao, Y. Chen, X. Huang, J. Xie, T.F. Shupe, Mater. Res. Express 7 (2020) 055302.
[46] R.K. Donato, A. Mija, Polymers (Basel) 12 (2020) 32.
[47] M. Prochon, G. Janowska, A. Przepiorkowska, A. Kucharska-Jastrzabek, J. Therm. Anal. Calorim. 109 (2012) 1563–1570.
[48] M. Brebu, I. Spiridon, J. Anal. Appl. Pyrolysis 91 (2011) 288–295.
[49] Y. Gao, S. Xu, Q. Yue, S. Ortaboy, B. Gao, Y. Sun, Adv. Powder Technol. 27 (2016) 1280–1286.
[50] G. Sanchez-Olivares, A. Sanchez-Solis, F. Calderas, J. Alongi, Polym. Degrad. Stabil. 140 (2017) 42–54.
[51] C. Lautenberger, J. Torero, C. Fernandez-Pello, V.B. Apte, in: Flammability Testing of Materials Used in Construction, Transport and Mining, Woodhead Publishing, Cambridge, UK, 2006, pp. 1–21.
[52] B. Schartel, R. Hull, Fire Mater. 31 (2007) 327–354.
[53] X. Hu, D. Wang, J. Appl. Polym. Sci. 129 (2013) 238–246.
[54] C.C. Höhne, R. Hanich, E. Kroke, Fire Mater. 42 (2018) 394–402.
[55] H.B. Chen, P. Shen, M.J. Chen, H.B. Zhao, D.A. Schiraldi, ACS Appl. Mater. Interfaces 8 (2016) 32557–32564.
[56] N. Wu, F. Niu, W. Lang, M. Xia, Carbohydr. Polym. 221 (2019) 221–230.
[57] Reaction-to-Fire Tests — Heat Release, Smoke Production and Mass Loss Rate, 2015 www.iso.org/standard/57957.html.
[58] T.K. Hong, B.S. Roh, S.H. Park, Energies 13 (2020) 2299.
[59] J. Alongi, A.R. Horrocks, F. Carosio, G. Malucelli, Update On Flame Retardant Textiles : State of the Art, Environmental Issues and Innovative Solutions, Smithers Rapra Publishing, Manchester, UK, 2013.
[60] E. Senoz, R.P. Wool, C.W.J. McChalicher, C.K. Hong, Polym. Degrad. Stabil. 97 (2012) 297–307.
[61] J. Albite-Ortega, S. Sánchez-Valdes, E. Ramírez-Vargas, F.J. Medellín-Rodríguez, L.F. Ramos deValle, O.S. Rodriguez-Fernandez, J.E. Rivera-Salinas, J.G. Martínez–Colunga, L. da-Silva, A.B. Morales-Cepeda, Z.V. Sanchez-Martínez, J.D. Zuluaga–Parra, Fire Mater. 47 (2023) 170–181.
[62] M. Ghanadpour, F. Carosio, L. Wågberg, Appl. Mater. Today 9 (2017) 229–239.
[63] F. Carosio, J. Alongi, G. Malucelli, Carbohydr. Polym. 88 (2012) 1460–1469.
[64] Y. Liu, Q.Q. Wang, Z.M. Jiang, C.J. Zhang, Z.F. Li, H.Q. Chen, P. Zhu, J. Anal. Appl. Pyrolysis 135 (2018) 289–298.